Free Radical Biology & Medicine 52 (2012) 1560–1568

Contents lists available at SciVerse ScienceDirect

Free Radical Biology & Medicine

journal homepage: www.elsevier.com/locate/freeradbiomed

Original Contribution

The glutathione disulfide mimetic NOV-002 inhibits cyclophosphamide-induced hematopoietic and immune suppression by reducing oxidative stress

C. Marcela Diaz-Montero [a,1,*], Yong Wang [b,1], Lijian Shao [c], Wei Feng [c], Abdel-Aziz Zidan [a], Christopher J. Pazoles [d], Alberto J. Montero [a], Daohong Zhou [b,c,**]

[a] Department of Medicine, Miller School of Medicine, University of Miami, Miami, FL 33136, USA
[b] Department of Pathology, Medical University of South Carolina, Charleston, SC 29425, USA
[c] Division of Radiation Health, Department of Pharmaceutical Sciences, University of Arkansas for Medical Sciences, Little Rock, AR 72205, USA
[d] Novelos Therapeutics, Newton, MA 02458, USA

ARTICLE INFO

Article history:
Received 7 June 2011
Revised 20 January 2012
Accepted 4 February 2012
Available online 15 February 2012

Keywords:
Glutathione disulfide
NOV-002
Cyclophosphamide
Oxidative stress
Reactive oxygen species
Free radicals

ABSTRACT

The oxidized glutathione mimetic NOV-002 is a unique anti-tumor agent that not only has the ability to inhibit tumor cell proliferation, survival, and invasion, but in some settings can also ameliorate cytotoxic chemotherapy-induced hematopoietic and immune suppression. However, the mechanisms by which NOV-002 protects the hematopoietic and immune systems against the cytotoxic effects of chemotherapy are not known. Therefore, in this study we investigated the mechanisms of action of NOV-002 using a mouse model in which hematopoietic and immune suppression was induced by cyclophosphamide (CTX) treatment. We found that NOV-002 treatment in a clinically comparable dose regimen attenuated CTX-induced reduction in bone marrow hematopoietic stem and progenitor cells (HSPCs) and reversed the immunosuppressive activity of myeloid-derived suppressor cells (MDSCs), which led to a significant improvement in hematopoietic and immune functions. These effects of NOV-002 may be attributable to its ability to modulate cellular redox. This suggestion is supported by the finding that NOV-002 treatment upregulated the expression of superoxide dismutase 3 and glutathione peroxidase 2 in HSPCs, inhibited CTX-induced increases in reactive oxygen species production in HSPCs and MDSCs, and attenuated CTX-induced reduction of the ratio of reduced glutathione to oxidized glutathione in splenocytes. These findings provide a better understanding of the mechanisms whereby NOV-002 modulates chemotherapy-induced myelosuppression and immune dysfunction and a stronger rationale for clinical utilization of NOV-002 to reduce chemotherapy-induced hematopoietic and immune suppression.

Many cancer patients receiving chemotherapy and/or radiotherapy develop hematopoietic and immune suppression that can lead to dose reductions and delays in therapy [1–4]. Dose reductions and treatment delays can compromise the outcomes of cancer therapy and decrease overall survival and disease-free survival [1,4–7]. However, strategies to effectively reduce the undesirable collateral effects of these therapies and accelerate the recovery of depressed hematopoietic and immune functions after chemotherapy and/or radiotherapy remain a major clinical problem.

An increasing body of evidence suggests that chemotherapy and radiation impair hematopoietic and immune functions not only by causing direct damage to DNA but also by increasing the production of reactive oxygen species (ROS) [8–12]. Increases in ROS production in hematopoietic stem and progenitor cells (HSPCs) can lead to bone marrow (BM) suppression through induction of HSPC apoptosis and senescence. The latter effect is primarily attributed to ROS-mediated stimulation of HSPC cycling and activation of the p38–p16 senescent pathway [13–20]. In addition, increased production of ROS is one of the key mechanisms by which myeloid-derived suppressive cells (MDSCs) inhibit various immune functions [21–30]. Therefore, antioxidant therapy has been proposed to have the potential to reduce chemotherapy- and radiation-induced hematopoietic and immune suppression. However, its use has been limited because of concerns that antioxidants can also compromise tumor cell response to chemotherapy and radiation.

NOV-002 is the oxidized form of glutathione disulfide (GSSG) that has exhibited significant anti-cancer activity when combined with cytotoxic chemotherapy (Fig. 1A) [31–36]. Interestingly, clinical and preclinical data also suggest that the addition of NOV-002 can reduce chemotherapy-induced hematologic toxicity and immune suppression [34,36]. Because of its potential hematopoietic promoting and

* Corresponding author. Fax: +1 305 243 5555.
** Correspondence to: D. Zhou, Department of Pathology, Medical University of South Carolina, Charleston, SC 29425, USA. Fax: +1 501 686 6517.
E-mail addresses: cdiaz1@med.miami.edu (C.M. Diaz-Montero), dzhou@uams.edu (D. Zhou).
[1] These authors contributed equally to this work.

0891-5849/$ – see front matter © 2012 Elsevier Inc. All rights reserved.
doi:10.1016/j.freeradbiomed.2012.02.007

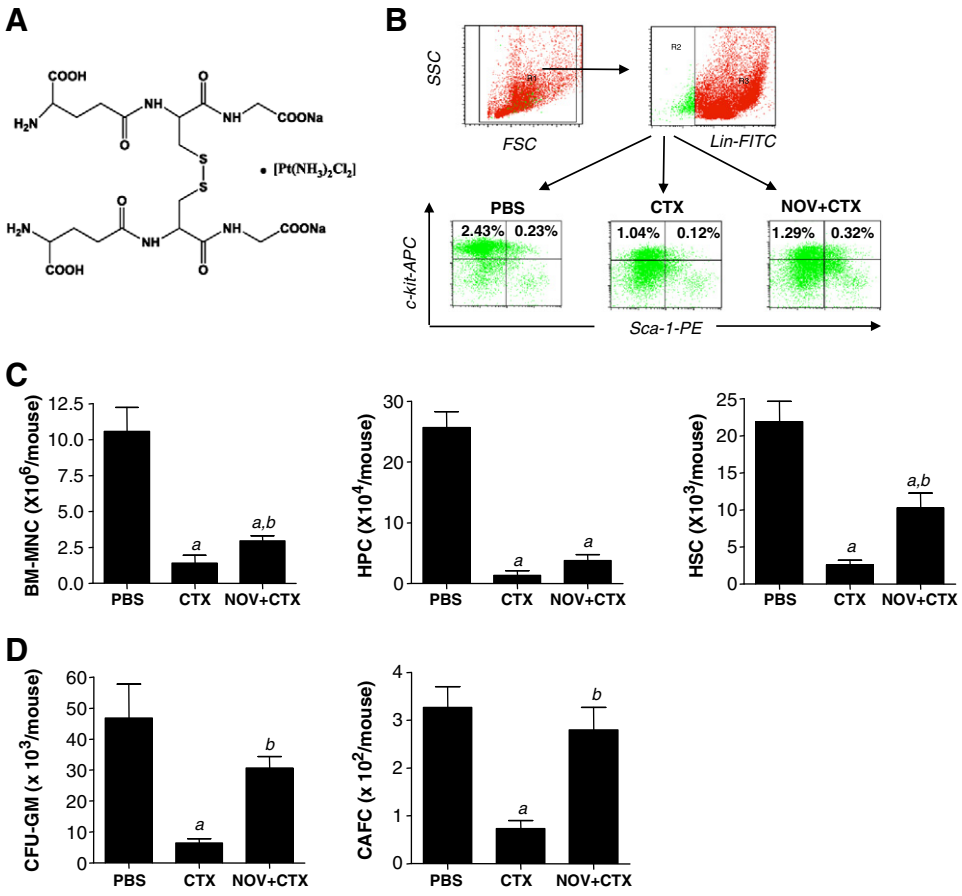

Fig. 1. NOV-002 reduces CTX-induced myeloid suppression. Mice were treated with vehicle (PBS), CTX alone (CTX), or CTX plus NOV-002 (NOV + CTX). Three days after treatment, BM cells were harvested for analyses of numbers and functions of HPCs and HSCs by flow cytometry and CFC and CAFC assays, respectively. (A) Structure of NOV-002. (B) Representative gating strategies for the analyses of HPCs (Lin^-, c-Kit^+, Sca-1^-) and HSCs (Lin^-, c-Kit^+, Sca-1^+) in BM-MNCs by flow cytometry. The numbers presented in the flow charts are the frequencies (%) of each cell population. (C) Average numbers of BM-MNCs, HPCs, and HSCs in each mouse. (D) Average numbers of CFU-GMs and day 35 CAFCs in each mouse. The data are presented as means ± SD of four or five independent experiments. $^a p<0.05$ vs PBS; $^b p<0.05$ vs CTX.

immunomodulatory activities, it has been suggested that NOV-002 may be particularly useful in combination with certain hematopoietic and immune suppressive chemotherapy agents such as cyclophosphamide (CTX) to treat cancer patients [36].

The mechanisms of action of NOV-002, however, in modulating the responses of the hematopoietic and immune systems to chemotherapy and/or radiotherapy have not been well characterized. It has been suggested that the pharmacologic effects of NOV-002 may be attributable to the modulation of cellular redox through its GSSG component [33,35,36]. Such modulation may underlie its clinical actions, including promotion of hematologic recovery and immunostimulation in the face of chemotherapy-induced hematopoietic and immune dysfunction that have been observed in some earlier studies [33,35,36]. To test this hypothesis, we examined the effects of NOV-002 on CTX-induced hematopoietic toxicity and immune suppression in a mouse model. Our results showed that NOV-002 treatment induced the expression of superoxide dismutase (SOD) 3 and glutathione peroxidase (GPX) 2 in HSPCs, inhibited CTX-induced increases in ROS production in HSPCs and MDSCs, and attenuated CTX-induced reduction in the ratio of reduced-to-oxidized glutathione in the spleen. These effects led to a significant improvement in hematopoietic and immune functions. These findings provide a better understanding of the mechanisms of action of NOV-002 in modulating chemotherapy-induced myelosuppression and immune dysfunction and provide a rationale of further clinical study of NOV-002 to promote BM recovery and enhance immunity during cytotoxic chemotherapy.

Materials and methods

Mice

Male C57BL/6 (Ly5.2) mice were purchased from The Charles River Laboratories (Wilmington, MA, USA). Mice were housed four in a cage and received food and water ad libitum. All mice were used at approximately 8–12 weeks of age. They were divided into three groups with a minimum of three to five mice per group: control, CTX, and NOV-002 plus CTX. Control mice were treated with phosphate-buffered saline (PBS) only, CTX mice were given an intraperitoneal (ip) injection of CTX (200 mg/kg; Sigma–Aldrich, St. Louis, MO, USA) on day 0, and NOV-002 plus CTX mice were treated with up to seven consecutive daily ip injections of 25 mg/kg NOV-002 (Novelos Therapeutics, Newton, MA, USA) starting on the day before CTX. At days 3 and 7 after CTX treatment, the mice were euthanized with CO_2 and by cervical dislocation for the collection of BM cells as described below. Pmel-1 transgenic (Ly5.2) mice originally obtained from The Jackson Laboratory (Bar Harbor, ME, USA) were bred in the AAALAC-certified animal facility of the Medical University of South Carolina (MUSC). T cells from Pmel-1 transgenic mice expressing the Vα1/Vβ13 T cell receptor specifically recognize the H-$2D^b$-restricted human $gp100_{25–33}$ epitope (KVPRNQDWL: $gp100_{25–33}$). This peptide represents an altered form of the murine $gp100_{25–33}$ (EGSRNQDWL) with improved binding to the MHC class I. The Institutional Animal Care and Use Committees of the MUSC and the

University of Miami approved all experimental procedures used in this study.

Isolation of bone marrow mononuclear cells (BM-MNCs) and preparation of splenocytes

The femora and tibiae were harvested from the mice immediately after they were euthanized. BM cells were flushed from the bones into Hanks' balanced salt solution containing 2% fetal calf serum using a 21-gauge needle and a 5-ml syringe. Cells from three to five mice were pooled to obtain a sufficient number of cells and centrifuged through Histopaque 1083 (Sigma–Aldrich) to isolate BM-MNCs. Spleen single-cell suspensions were prepared as previously described [20,37].

Quantitative analysis of BM hematopoietic stem cells (HSCs) and hematopoietic progenitor cells (HPCs)

Briefly, 1×10^6 BM-MNCs were incubated with biotin-conjugated rat antibodies against CD3 , CD45R/B220, Gr-1, Mac-1, and Ter-119 and then with streptavidin–FITC. After incubation with anti-CD16/CD32 antibody, they were stained with anti-Sca-1–PE and anti-c-kit–APC antibodies. All these antibodies were purchased from BD Biosciences (San Diego, CA, USA). Lin^-, c-Kit^+, Sca-1^+ cells represent enriched HSCs and Lin^-, c-Kit^+, Sca-1^- cells are HPCs. For each sample, a minimum of 200,000 cells were analyzed on a FACSCalibur (Becton–Dickinson, San Jose, CA, USA), and the data were analyzed using CellQuest software (Becton–Dickinson) after gating on viable cells.

Colony-forming cell (CFC) assay

Colony-forming unit–granulocyte macrophage (CFU-GM) was analyzed by CFC assay to measure HPC function. Briefly, BM-MNCs were suspended in MethocultM3434 medium (StemCell Technologies, Vancouver, BC, Canada) at 2×10^4 viable cells/ml and seeded in wells of 24-well plates. The plates were incubated at 37 °C in a humidified incubator with 5% CO_2 in air for 7 days. Colonies of 50 or more cells were scored under an inverted microscope.

Cobblestone area-forming cell (CAFC) assay

The CAFC assay was done according to the procedures developed by Pleomacher et al. with modifications as we previously reported [37–39]. Briefly, stromal layers were prepared by seeding 10^3 FBMD-1 stromal cells per well into flat-bottom 96-well plates (Falcon, Lincoln Park, NJ, USA). One week later, BM-MNCs were overlaid on these stromal layers in six dilutions, threefold apart, consisting of 20 wells per dilution to allow limiting-dilution analysis of the precursor cells forming hematopoietic clones under the stromal layer. Cultures were fed weekly by changing half of the medium. The frequencies of CAFCs were determined at 35 days of culture to measure the clonogenic function of HSCs as previously described [37–39].

Analysis of the frequencies of erythroid progenitors in BM-MNCs by flow cytometry

Briefly, 1×10^6 BM-MNCs were incubated with anti-CD16/CD32 antibody (BD Biosciences) to block antibody-nonspecific bindings. The cells were then stained with PE-conjugated Ter-199 antibody (BD Biosciences) to label erythroid progenitors. Phenotypic analysis of erythroid progenitors was performed using a FACSCalibur (Becton–Dickinson) and the data were analyzed using CellQuest software (Becton–Dickinson) after gating on viable cells.

Analysis of ROS production in BM HSPCs

BM lineage-negative hematopoietic cells (Lin^- cells) were isolated as described previously [8,9]. Lin^- cells (1×10^6/ml) stained with anti-Sca-1–PE and anti-c-Kit–APC antibodies were suspended in PBS supplemented with 5 mM glucose, 1 mM $CaCl_2$, 0.5 mM $MgSO_4$, and 5 mg/ml bovine serum albumin and then incubated with 5-(and-6)-chloromethyl-2′,7′-dichlorodihydrofluorescein diacetate (CM-H_2DCFDA; Invitrogen, Carlsbad, CA, USA) (10 μM) for 30 min at 37 °C. The levels of ROS in Lin^- cells, HPCs, and HSCs were analyzed by measuring the mean fluorescence intensity (MFI) of 2′,7′-dichlorofluorescein (DCF) using a FACSCalibur flow cytometer (Becton–Dickinson). For each sample, a minimum of 200,000 Lin^- cells was acquired and the data were analyzed using CellQuest software (Becton–Dickinson). In all experiments, PE and APC isotype controls and other positive and negative controls were included as appropriate.

Analysis of the frequencies of MDSCs in peripheral blood and the spleen by flow cytometry

Peripheral blood and cell suspensions from spleens were incubated with APC-conjugated anti-CD11b and PE-conjugated anti-Ly6G antibodies (BD Biosciences). The percentage of double-positive cell population was determined using a FACSCalibur flow cytometer (Becton–Dickinson). For each sample, a minimum of 200,000 events were acquired and the data were analyzed using CellQuest software (Becton–Dickinson).

In vitro T cell suppression assay

Splenocytes were incubated with APC-conjugated anti-CD11b and PE-conjugated anti-Ly6G antibodies (BD Biosciences). $CD11b^+$, $Ly6G^+$ MDSCs were isolated by cell sorting using an Aria cell sorter (BD Biosciences). $CD3^+$ T cells were isolated using magnetic beads (BD Biosciences) following the manufacturer's instructions. MDSCs and T cells were cocultured at the indicated ratios and stimulated with anti-CD3/CD28-coated beads (BD Biosciences) at 1/1 bead-to-T-cell ratio. Five days after culture, the cells were pulsed with [^{3}H] thymidine overnight and the incorporation of [^{3}H]thymidine was determined by a scintillation counter. Percentage suppression of T cell proliferation was calculated as (cpm from wells containing MDSCs × 100)/(cpm from wells without MDSCs).

In vivo T cell suppression assay

C57BL/6 mice ($Ly5.2^+$) were treated with PBS, CTX, or NOV-002 and CTX as described previously. At day 7 after CTX injection 1×10^7splenocytes from Pmel mice ($Ly5.1^+$) were adoptively transferred to these mice. The recipient mice were vaccinated with 100 μg of mouse $gp100_{25-33}$ melanoma peptide24 h after the cell transfer. The frequencies of transferred Pmel T cells were determined 3 days after vaccination by flow cytometry to detect $Ly5.1^+$ donor T cells.

Analysis of ROS production in MDSCs

Briefly, BM cells were incubated at 37 °C in the presence of 5 μM CM-H_2DCFDA for 30 min after immunostaining with APC-conjugated anti-CD11b and PE-conjugated anti-Ly6G antibodies (BD Biosciences). For induced activation, cells were cultured simultaneously with CM-H_2DCFDA and 30 ng/ml phorbol myristate acetate (PMA; Sigma–Aldrich). Analysis of ROS production in $CD11b^+$, $Ly6G^+$ MDSCs was then conducted by flow cytometry as described above.

Analysis of reduced glutathione (GSH)-to-oxidized glutathione (GSSG) ratio

Spleen sections from the same mice were cryopreserved in PBS (GSH sample) or in 30 μl of scavenger solution (GSSG sample) (Oxford Biomedical Research, Rochester Hills, MI, USA). The amounts of GSH and GSSG were assayed using a microplate assay kit (Oxford Biomedical Research) after thawing and deproteination with a 5% metaphosphoric acid solution. Concentrations of GSH and GSSG were extrapolated from a calibration curve and the ratio was calculated as follows: ratio = $GSH_t - 2GSSG/GSSG$.

Analysis of mRNA expression of antioxidant enzymes in HSPCs by real-time RT-PCR

Total RNA was extracted from purified HSPCs (Lin^-, c-Kit^+, Sca-1^+ cells) using the RNeasy Mini Kit (Qiagen, Valencia, CA, USA) according to the manufacturer's instructions. First-strand cDNA was synthesized from total RNA using the SuperScript II first-strand synthesis system (Invitrogen) as we previously described. PCR primers for SOD1, SOD2, SOD3, catalase, GPX1, GPX2, peroxiredoxin (PRDX) 1, PRDX2, and thioredoxin reductase (TXNRD) 1 were customer-designed and obtained from Integrated DNA Technologies (Coralville, IA, USA). The sequences of the primers are listed in Table 1. The threshold cycle (C_t) value for each gene was normalized to the C_t value of glyceraldehyde-3-phosphate dehydrogenase. The relative mRNA expression was calculated using the comparative C_t ($2^{-\Delta\Delta Ct}$) method.

Statistical analyses

Statistical analyses were performed using two-sided *t* test and nonparametric Mann–Whitney *U* test. Differences were considered significant at $p<0.05$. All of the analyses were done using GraphPad Prism from GraphPad Software, Inc. (San Diego, CA, USA).

Results

NOV-002 reduces CTX-induced myelosuppression by protecting HSPCs

To elucidate the mechanisms by which NOV-002 reduces chemotherapy-induced BM toxicity, we first examined the effects of NOV-002 treatment on CTX-induced myelosuppression using a murine model. In this model, mice were given a single dose of CTX with or without daily NOV-002 injections starting on the day before chemotherapy. This daily regimen closely resembles the dosing schedule of NOV-002 utilized in clinical trials. On day 3 after CTX treatment, the mice were sacrificed and BM cells were harvested. The frequencies of HSCs (Lin^-, c-Kit^+, Sca-1^+ cells) and HPCs (Lin^-, c-Kit^+, Sca-1^- cells) in BM-MNCs were analyzed by flow cytometry (Fig. 1B). The number of these cells was calculated according to the total number of BM-MNCs and averaged for each mouse in the same treatment groups. An initial experiment showed that mice treated with NOV-002 alone did not exhibit any significant changes in various BM indices compared with vehicle-treated controls (data not shown). Therefore, in the subsequent experiments, this group was omitted from the study. As shown in Fig. 1C, treatment with CTX resulted in a significant reduction in the numbers of BM-MNCs, HPCs, and HSCs. This reduction was attenuated by treatment with NOV-002. To test if the clonogenic function of HPCs and HSCs can also be protected by NOV-002 treatment, we performed CFU-GM and CAFC assays, respectively. In concordance with our previous findings, CTX significantly reduced the clonogenic functions of both HPCs and HSCs [9]. However, daily NOV-002 injections resulted in significantly higher levels of HSC clonogenic function as measured by day 35 CAFCs compared to CTX alone. Likewise, the levels of HPC clonogenic function measured by CFU-GMs were also significantly higher in NOV-002-treated mice than in CTX alone-treated mice, but to a lesser extent than that observed with HSCs (Fig. 1D).

Because some previous clinical studies with NOV-002 in cancer patients receiving chemotherapy have reported a decrease in anemic events [36,40], we examined whether NOV-002 treatment had an effect on the CTX-induced damage to erythroid precursors. To this end, BM cell suspensions were harvested from mice on day 3 after PBS or CTX injection with or without NOV-002 treatment. The cells were stained with an antibody against the erythroid marker Ter-119. Fig. 2A shows a representative dot plot of BM cells from each experimental group. We found significantly higher levels of Ter-119-positive cells in BM cells from NOV-002-treated mice at day 3 post-CTX relative to mice that received CTX only (Fig. 2B). Greater numbers of megakaryocyte–erythrocyte progenitors, which give rise to megakaryocyte–erythrocyte lineages, were also observed in BM of mice treated with NOV-002 on day 3 after CTX treatment than in those of mice with CTX treatment alone (data not shown). Taken together, these data suggest that NOV-002 treatment can ameliorate CTX-induced BM toxicity not only by reducing the decrease in HSCs and HPCs, but also by preserving their hematopoietic function.

NOV-002 inhibits CTX-induced increase in ROS production in HSPCs

Increases in ROS production in HSPCs can occur under various pathological conditions that lead to inhibition of HSPC function and BM suppression, because ROS can induce HSPC apoptosis and senescence in a dose-dependent manner [13–20]. We examined whether NOV-002 as a redox modulator can reduce CTX-induced BM suppression in part by downregulating ROS production in HSPCs. As shown in Fig. 3, the MFI of DCF in Lin^- BM hematopoietic cells, HPCs, and HSCs from CTX-treated animals was significantly greater than that in the cells from PBS-treated mice. This change is unlikely to be caused by the differences in the uptake of CM-H_2DCFDA and efflux of DCF between the cells from PBS-treated mice and those from CTX-treated animals, as they showed similar DCF MFI after the cells were incubated with irradiated CM-H_2DCFDA (data not shown). In addition, Mn(III) *meso*-tetrakis(*N*-ethylpyridinium-2-yl) porphyrin, a superoxide dismutase mimetic and potent antioxidant, could inhibit CTX-induced increases in DCF MFI in HSPCs (data not shown). These results suggest that CTX treatment elevates ROS production in hematopoietic cells. Interestingly, the increases were abrogated in HSCs and attenuated in Lin^- cells and HPCs by the treatment with NOV-002. These results demonstrate that indeed NOV-002 has the ability to reduce CTX-induced

Table 1
Primer sequences used for real-time RT-PCR.

Gene	GenBank Accession No.	Sequence of oligonucleotide primer
SOD1	NM_011434	S: 5′-GTATGGGGACAATACACAAGGCTGTAC-3′ A: 5′-AATGCTCTCCTGAGAGTGAGATCACAC-3′
SOD2	NM_013671	S: 5′-CACATTAACGCGCAGATCATGCAG-3′ A: 5′-ACCTGAGTTGTAACATCTCCCTTG-3′
SOD3	NM_011435	S: 5′-ATGGAGCTAGGACGACGAAGGGAG-3′ A: 5′-AGACTGAAATAGGCCTCAAGCCTG-3′
Catalase	NM_009804	S: 5′-TGCAAGTTCCATTACAAGACCGACCAG-3′ A: 5′-ACGTCCAGGACGGGTAATTGCCATTGG-3′
GPX1	NM_008160	S: 5′-TCAGTTCGGACACCAGGAGAATGG-3′ A: 5′-CACTGGGTGTTGGCAAGGCATTCC-3′
GPX2	NM_030677	S: 5′-AACCAGTTCGGACATCAGGAGAAC-3′ A: 5′-GGCAAAGACAGGATGCTCGTTCTG-3′
PRDX1	NM_011034	S: 5′-GTCATCTGGCATGGATTAACACAC-3′ A: 5′-CCCTGAAAGAGATACCTTCATCAG-3′
PRDX2	NM_011563	S: 5′-CACCCACCTGGCGTGGATCAATAC-3′ A: 5′-AAAGAGACCCCTGTAAGCAATGCC-3′
TXNRD1	NM_001042513	S: 5′-CCTCTTGGGACCAGATGGGGTCTC-3′ A: 5′-CCAGTCATGCTTCACTGTGTCTTC-3′
HPRT	NM_013556	S: 5′-AGCAGTACAGCCCCAAAATGGTTA-3′ A: 5′-TCAAGGGCATATCCAACAACAAAC-3′

S, sense; A, antisense.

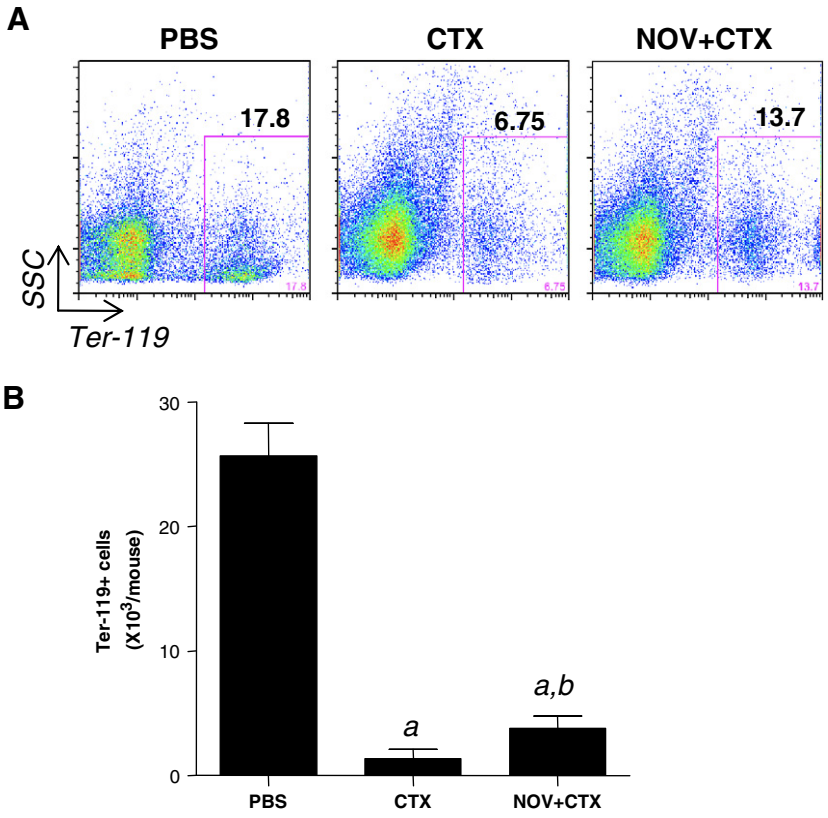

Fig. 2. NOV-002 protects erythrocyte precursors against CTX-induced toxicity. Mice were treated with vehicle (PBS), CTX alone (CTX), or CTX plus NOV-002 (NOV + CTX). Three days after treatment, BM cells were harvested for analysis of Ter-119$^+$ erythroid cells. (A) Representative gating strategies for the analysis of Ter-119$^+$ erythroid cells in BM-MNCs by flow cytometry. The numbers presented in the scatter plots are the frequencies (%) of Ter-119$^+$ erythroid cells in BM-MNCs. (B) Average numbers of BM Ter-119$^+$ cells in each mouse. The data are presented as means ± SD of three independent experiments. $^a p<0.05$ vs PBS; $^b p<0.05$ vs CTX.

increase in ROS production in HSPCs, which may confer a significant protection of HSPCs against CTX-induced toxicity.

NOV-002 does not reduce the induction of MDSCs by CTX, but decreases their immunosuppressive activity

Our group and others have previously reported that CTX treatment can increase circulating MDSCs (CD11b$^+$, Ly6G$^+$ cells) in both mice and humans [22,41–46]. MDSCs are strong suppressors of T-cell-mediated responses [28,47] and therefore may contribute to CTX-induced immune suppression [46]. We examined if the treatment with NOV-002 can also have an impact on CTX-induced immune suppression by modulating the induction and activity of MDSCs. As shown in Fig. 4A, CTX significantly increased the frequencies of MDSCs in the spleen and peripheral blood. The increases were not affected by NOV-002 treatment. We then determined whether NOV-002 treatment had an effect on the immunosuppressive activity of MDSCs. To this end, T cells were cocultured with purified MDSCs at various T-cell-to-MDSC ratios and then activated with beads coated with monoclonal antibodies against CD3 and CD28. The proliferation of T cells was determined by [^{3}H]thymidine incorporation, and the percentage suppression of T cell proliferation was calculated relative to the proliferation observed in the absence of MDSCs. Fig. 4B shows a significant decrease in the percentage of suppression of T cell proliferation by MDSCs isolated from mice treated with CTX + NOV-002 compared with MDSCs isolated from mice treated with CTX only.

Next, we examined the effect of NOV-002 treatment on the in vivo immunosuppressive activity of CTX-induced MDSCs. In this study, C57BL/6 (Ly5.2) mice were injected with PBS, CTX, or CTX + NOV-002 as described before. After 7 days of treatment, 1×10^7 splenocytes from Pmel mice (Ly5.1$^+$) were adoptively transferred to the treated mice. One day after transfer, the recipient mice received 100 μg of cognate gp100 peptide, and 3 days later the frequency of Pmel cells in the peripheral blood was determined by flow cytometry according to Ly5.1 staining among host lymphocytes as shown in Fig. 4C. Fig. 4D shows a robust expansion of Pmel lymphocytes in response to activation with cognate peptide in mice that did not receive CTX. However, this expansion was significantly reduced after CTX treatment presumably because of the suppressive effect of CTX-derived MDSC [23,28,29]. By contrast, daily NOV-002 injections after CTX treatment were able to attenuate the reduction in Pmel cell expansion. These results suggest that NOV-002, although unable to alter the overall expansion of CTX-induced MDSCs as shown in Fig. 4C, is able to reduce their ability to suppress T cell responses.

NOV-002 treatment inhibits ROS production by CTX-induced MDSCs and increases GSH/GSSG ratio in MDSCs from CTX-treated mice

To further elucidate the mechanism associated with the reduction in the immunosuppressive activity of CTX-induced MDSCs after NOV-002 treatment, we measured the levels of ROS in MDSCs from mice treated with CTX or CTX + NOV-002, because it has been suggested that increased production of ROS can increase the immunosuppressive activity of MDSCs [23,28–30]. ROS production by MDSCs from mice receiving CTX and/or NOV-002 treatment was determined by flow cytometry with or without PMA stimulation as shown in Fig. 5A. Treatment of mice with NOV-002 significantly reduced ROS production in unstimulated MDSCs from CTX-treated mice by approximately 44%. As expected, stimulation of MDSCs from day 7 CTX-treated mice with PMA (30 ng/ml) led to a further increase in

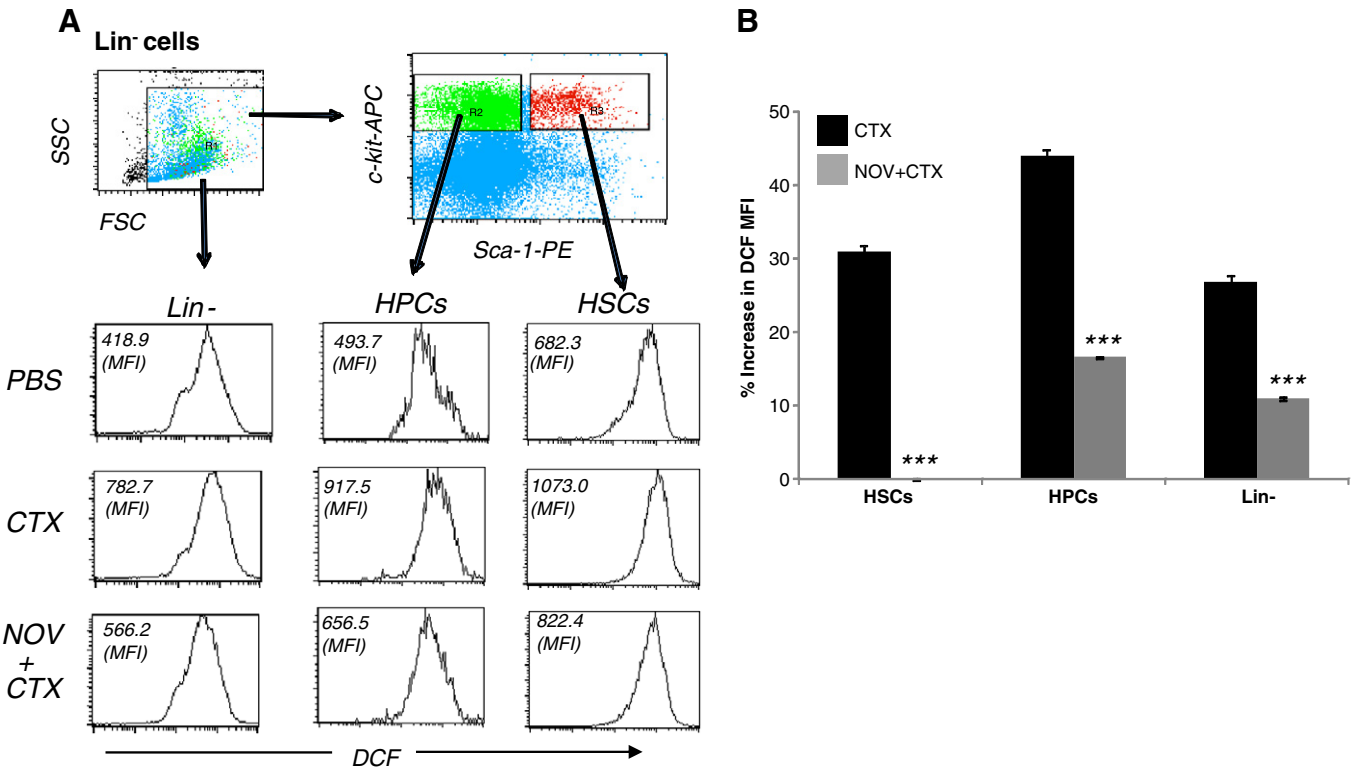

Fig. 3. NOV-002 inhibits CTX-induced ROS production in BM HSPCs. Mice were treated with vehicle (PBS), CTX alone (CTX), or CTX plus NOV-002 (NOV + CTX). Three days after treatment, BM cells were harvested and analyzed. (A) Representative analysis of ROS production in BM lineage-negative hematopoietic cells (Lin^-), HPCs, and HSCs by flow cytometry. The numbers presented in the scatter plots are the mean fluorescence intensity of DCF. (B) Percentage increase in ROS production by Lin^- cells, HPCs, and HSCs after treatment with CTX or CTX plus NOV-002 compared to PBS-treated cells according to the changes in DCF MFI. The data are presented as means ± SD of three independent experiments. $^{***}p<0.05$ vs CTX.

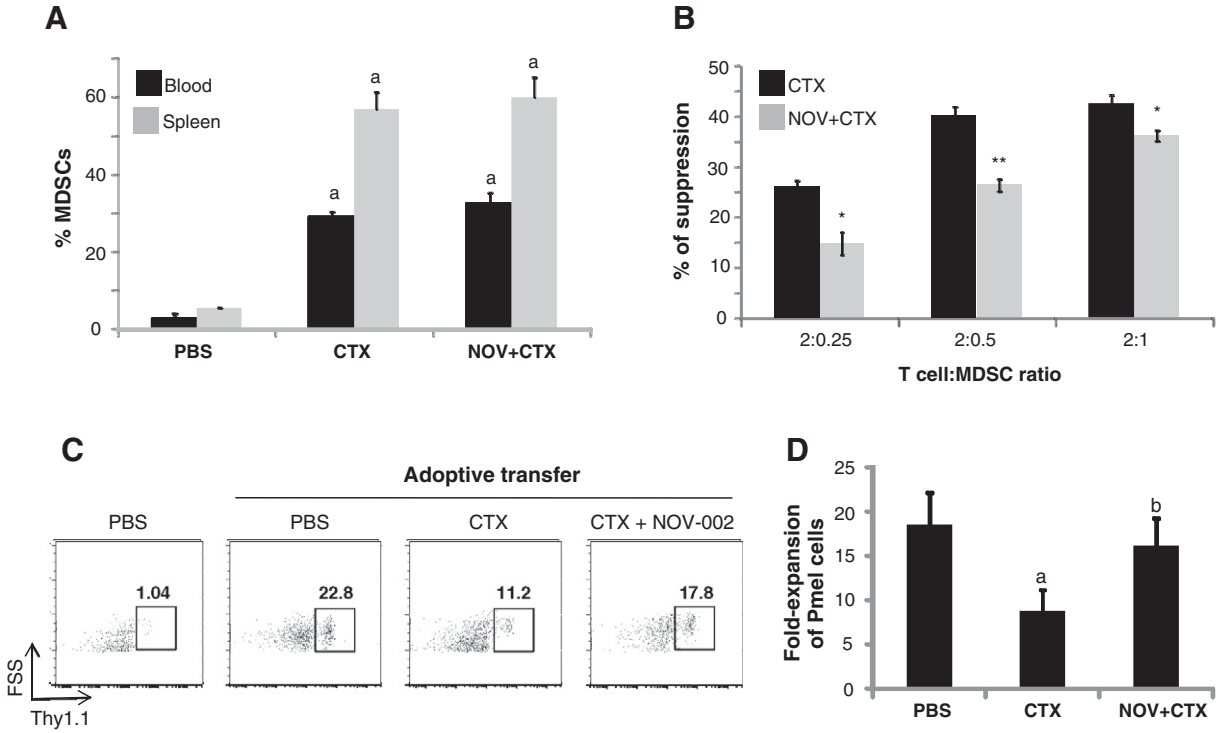

Fig. 4. NOV-002 does not reduce the induction of MDSCs by CTX but decreases their immunosuppressive activity. Mice were treated with vehicle (PBS), CTX alone (CTX), or CTX plus NOV-002 (NOV + CTX). Seven days after treatment, peripheral blood cells and splenocytes were harvested for analysis of $CD11b^+$, $Ly6G^+$ MDSCs by flow cytometry. (A) Percentages of MDSCs in peripheral blood cells and splenocytes. The data are presented as means ± SD of three independent experiments. $^a p<0.05$ vs PBS. (B) Percentage suppression of in vitro T cell proliferation by MDSCs isolated from the spleens of mice treated with CTX or NOV-002 + CTX. The data are presented as means ± SD of three independent experiments. $^*p=0.05$ and $^{**}p=0.01$ vs CTX. (C) Gating strategy to determine the expansion of donor-derived Pmel T cells ($Thy1.1^+$) after adoptive transfer and vaccination. The numbers presented in the scatter plots are the frequencies (%) of donor-derived Pmel T cells in the spleen Thy1.1-positive T cells. (D) Fold increase in the expansion of donor-derived Pmel T cells after vaccination compared to mice without adoptive transfer. The data are presented as means ± SD of five independent experiments. $^a p<0.02$ vs PBS; $^b p<0.01$ vs CTX.

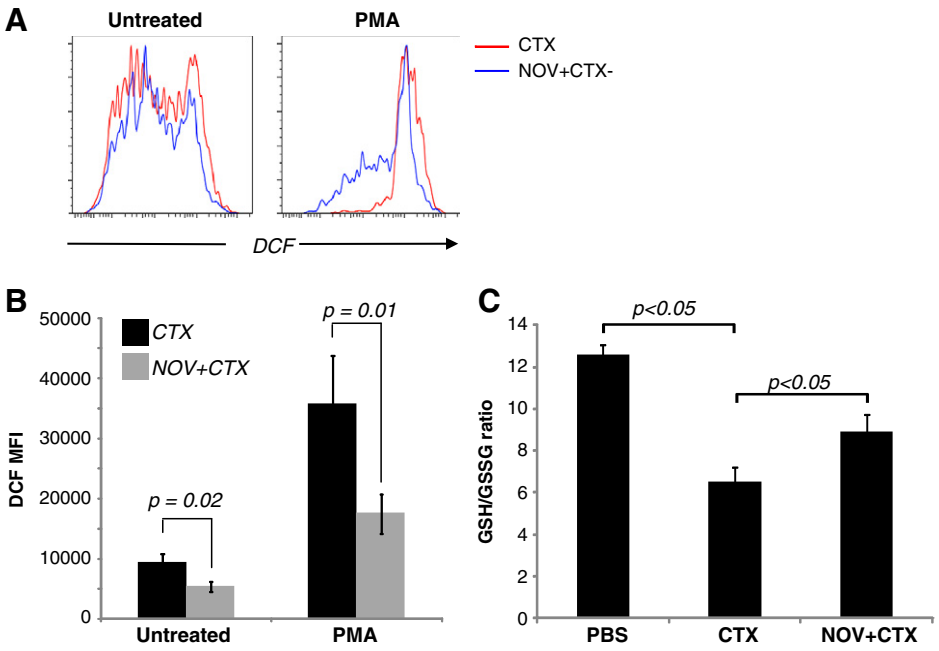

Fig. 5. NOV-002 treatment inhibits ROS production by CTX-induced MDSCs and associates with an increase in the GSH/GSSG ratio in splenocytes from CTX-treated mice. Mice were treated with CTX alone (CTX) or CTX plus NOV-002 (NOV + CTX). Seven days after treatment, ROS production in BM $CD11b^+$, $Ly6G^+$ MDSCs with or without PMA stimulation was determined by flow cytometry and the levels of GSH and GSSG in splenocytes without PMA stimulation were quantified for calculation of the GSH/GSSG ratio. (A) Representative analyses of ROS production in BM $CD11b^+$, $Ly6G^+$ MDSCs by flow cytometry. (B) Average ± SD ($n = 5$) of DCF MFI from untreated or PMA-activated MDSCs isolated from BM. (C) Average ± SD ($n = 5$) of the GSH/GSSG ratio in splenocytes from mice treated with PBS, CTX alone, or CTX plus NOV-002.

ROS production. However, the increase again was significantly reduced by NOV-002 treatment (Fig. 5B). In addition, we analyzed the overall levels of GSH and GSSG in spleen and calculated their ratio and found that CTX treatment significantly reduced the GSH/GSSG, whereas NOV-002 treatment attenuated the reduction (Fig. 5C). These results suggest that treatment with NOV-002 decreases the production of ROS by CTX-induced MDSCs, which may contribute to the reversal of MDSC-mediated immune suppression of T cell function.

NOV-002 treatment increases SOD3 and GPX2 expression in HSPCs

To gain more insight into the mechanisms by which NOV-002 regulates ROS production in HSPCs after CTX treatment, we analyzed the mRNA expression of several important antioxidant enzymes by real-time RT-PCR. As shown in Fig. 6, the expression of SOD3 and GPX2 mRNA in HSPCs was downregulated more than 50% by the treatment with CTX, whereas the expression of all other antioxidant enzymes examined was not significantly changed by CTX injection. The downregulation of the expression of SOD3 and GPX2 mRNA in HSPCs was completely inhibited by NOV-002 treatment. More interestingly, the expression of SOD3 mRNA was actually increased about 2.5-fold in the cells from NOV-002-treated mice compared to that in the cells from PBS-treated mice. These findings suggest that NOV-002 can inhibit CTX-induced oxidative stress in HSPCs at least in part by upregulating the expression of SOD3 and GPX2.

Discussion

Hematologic toxicity and immune suppression are common complications of chemotherapy in cancer patients [6,48]. The mechanisms by which chemotherapeutic agents cause these complications are not yet completely understood, but may be attributed in part to the induction of increased production of ROS in HSPCs [49–54] and MDSCs [23,29].

It has been well established that increased production of ROS contributes to the BM suppression induced by total body irradiation [9]. However, the role of ROS in mediating BM suppression induced by chemotherapeutic agents such as CTX was not well understood. Our present studies suggest that ROS may also play an important role in CTX-induced myelosuppression. First, we have found that increased production of ROS is associated with CTX-induced hematopoietic

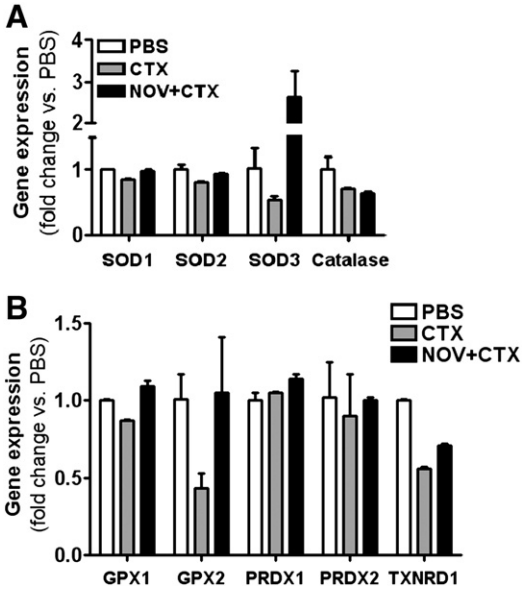

Fig. 6. Effects of NOV-002 treatment on the expression of selected antioxidant enzyme mRNAs in HSPCs. Mice were treated with vehicle (PBS), CTX alone (CTX), or CTX plus NOV-002 (NOV + CTX). Three days after treatment, HSPCs were purified by cell sorting and their expression of selected antioxidant enzyme mRNAs was quantified by real-time RT-PCR. The data are presented as means ± SD of fold changes vs PBS-treated cells ($n = 3$).

toxicity. Furthermore, our study shows that the addition of the glutathione disulfide mimetic NOV-002 to CTX, a widely used chemotherapeutic agent, results in protection of BM HSPCs against the cytotoxic effects of CTX, including the preservation of the number of BM HSPCs and their clonogenic activities. The protective effects of NOV-002 against CTX may be attributable to its ability to modulate cellular redox. This suggestion is supported by the finding that NOV-002 treatment upregulated the expression of SOD3 and GPX2 in HSPCs, inhibited CTX-induced increases in ROS production in HSPCs and MDSCs, and attenuated CTX-induced reduction in the ratio of GSH/GSSG in MDSCs. However, the mechanisms by which ROS mediate CTX-induced HSPC injury have yet to be elucidated. However, it has been shown that ROS can impair HSPC function by inducing HSPC apoptosis and senescence. The induction of HSPC apoptosis is primarily attributed to ROS-produced oxidative damage. In contrast, the induction of HSPC senescence may result from ROS-mediated stimulation of constant HSPC cycling and activation of the p38 mitogen-activated protein kinase–$p16^{Ink4a}$ pathway. It has yet to be determined whether CTX causes BM suppression through induction of HSPC apoptosis and/or senescence through ROS. In addition, it appears that the protective effect of NOV-002 on HSCs was greater than that on HPCs as shown in Figs. 1C and D. This may be attributable to the higher sensitivity of HSCs to oxidative damage compared to HPCs as shown in previous studies [9,15–17]. Although NOV-002 can effectively protect HSPCs by inhibiting CTX-induced ROS production, it is unlikely that NOV-002 will increase the risk of cancer patients to secondary malignancies. This is because it has been well established that increase in ROS production is the underlying mechanism whereby chemotherapy and radiation cause genetic instability that can lead to the induction of leukemia and cancer.

MDSCs are a heterogeneous population of immature myeloid cells whose numbers can increase rather dramatically in a variety of diseases, including cancer, autoimmune disease, trauma, burns, and sepsis, as well as in response to certain immunosuppressive chemotherapeutic drugs, such as CTX [21–23,28,29]. Initial studies on MDSCs have occurred mostly in the setting of cancer, focusing on the ability of MDSCs to suppress T cell activation through several mechanisms, including generation of ROS, depletion of GSH, nitrosylation of T cell receptor, depletion of extracellular arginine (essential micronutrient for T cells), and secretion of immune-inhibitory cytokines and molecules (such as IL-10 and prostaglandins) [21–30]. Our group and others have previously shown an association between CTX-containing chemotherapy and increased levels of circulating MDSCs, which can suppress T cell activation in various preclinical and clinical settings [22,42–45]. Our results presented here showed that NOV-002 had no impact on overall levels of CTX-induced MDSCs. However, MDSCs from mice treated with NOV-002 showed decreased immunosuppressive capabilities. Because one of the immunosuppressive mechanisms of MDSCs is the generation of ROS, we examined whether NOV-002 affected the ability of MDSCs to generate ROS. Our findings suggest that daily treatment with NOV-002 was able to reverse T cell suppression by CTX-derived MDSCs in vivo, through downregulation of ROS production as seen in HSCs/HPCs.

These findings suggest that pharmacological modulators of the redox pathway, such as NOV-002, may be an alternative to growth factors for ameliorating chemotherapy-induced hematologic toxicities and immune suppression. This is particularly important when concerns about widespread use of erythropoiesis-stimulating agents decreasing survival and/or leading to poorer cancer-related outcomes in cancer patients have restricted their use, and no other alternatives currently exist other than blood transfusions. Moreover, our results also demonstrate that NOV-002 was able to modulate the suppressive effects of CTX-derived MDSCs. These studies further our understanding of the hematologic effects of NOV-002. One previous randomized phase 2 trial in patients with advanced non-small-cell lung cancer receiving platinum-based chemotherapy ± daily NOV-002 injections reported that patients receiving NOV-002 in combination with chemotherapy had reduced hematologic toxicities from the chemotherapy as evidenced by significantly higher peripheral leukocyte, hemoglobin, and lymphocyte counts [36]. However, these findings were not observed in a subsequent larger randomized phase 3 trial. Our results here suggest that this improvement in hematologic indices by the addition of daily NOV-002 observed in some clinical trials may be attributable in part to the ability of this compound to inhibit ROS production in HSPCs in response to chemotherapy. However, unlike other redox-modulating agents, particularly various antioxidants, NOV-002 does not protect tumor cells against chemotherapy. Therefore, NOV-002 may be of particular benefit in the amelioration of chemotherapy-induced hematologic toxicities and immune suppression in cancer patients.

Acknowledgments

The authors thank Mrs. Aimin Yang for her excellent technical assistance and Mr. Richard Peppler and Dr. Haiqun Zeng at the Hollings Cancer Center Flow Cytometry & Cell Sorting Shared Resource for the flow cytometric analysis and cell sorting. This study was supported in part by grants from the National Institute of Allergy and Infectious Diseases and the National Cancer Institute.

References

[1] Herbst, C.; Naumann, F.; Kruse, E. B.; Monsef, I.; Bohlius, J.; Schulz, H.; Engert, A. Prophylactic antibiotics or G-CSF for the prevention of infections and improvement of survival in cancer patients undergoing chemotherapy. *Cochrane Database Syst. Rev.*CD007107; 2009.
[2] Daniel, D.; Crawford, J. Myelotoxicity from chemotherapy. *Semin. Oncol.* **33:** 74–85; 2006.
[3] Weycker, D.; Malin, J.; Edelsberg, J.; Glass, A.; Gokhale, M.; Oster, G. Cost of neutropenic complications of chemotherapy. *Ann. Oncol.* **19:**454–460; 2008.
[4] Lyman, G. H.; Michels, S. L.; Reynolds, M. W.; Barron, R.; Tomic, K. S.; Yu, J. Risk of mortality in patients with cancer who experience febrile neutropenia. *Cancer* **116:**5555–5563; 2010.
[5] Hershman, D. L.; Wang, X.; McBride, R.; Jacobson, J. S.; Grann, V. R.; Neugut, A. I. Delay of adjuvant chemotherapy initiation following breast cancer surgery among elderly women. *Breast Cancer Res. Treat.* **99:**313–321; 2006.
[6] Bohlius, J.; Herbst, C.; Reiser, M.; Schwarzer, G.; Engert, A. Granulopoiesis-stimulating factors to prevent adverse effects in the treatment of malignant lymphoma. *Cochrane Database Syst. Rev.*CD003189; 2008.
[7] Bohlius, J.; Tonia, T.; Schwarzer, G. Twist and shout: one decade of meta-analyses of erythropoiesis-stimulating agents in cancer patients. *Acta Haematol.* **125:** 55–67; 2011.
[8] Naka, K.; Hirao, A. Maintenance of genomic integrity in hematopoietic stem cells. *Int. J. Hematol.* **93:**434–439; 2011.
[9] Wang, Y.; Liu, L.; Pazhanisamy, S. K.; Li, H.; Meng, A.; Zhou, D. Total body irradiation causes residual bone marrow injury by induction of persistent oxidative stress in murine hematopoietic stem cells. *Free Radic. Biol. Med.* **48:**348–356; 2010.
[10] Prus, E.; Fibach, E. Effect of iron chelators on labile iron and oxidative status of thalassaemic erythroid cells. *Acta Haematol.* **123:**14–20; 2010.
[11] Ghaffari, S. Oxidative stress in the regulation of normal and neoplastic hematopoiesis. *Antioxid. Redox Signal.* **10:**1923–1940; 2008.
[12] Naka, K.; Muraguchi, T.; Hoshii, T.; Hirao, A. Regulation of reactive oxygen species and genomic stability in hematopoietic stem cells. *Antioxid. Redox Signal.* **10:** 1883–1894; 2008.
[13] Hole, P. S.; Pearn, L.; Tonks, A. J.; James, P. E.; Burnett, A. K.; Darley, R. L.; Tonks, A. Ras-induced reactive oxygen species promote growth factor-independent proliferation in human CD34+ hematopoietic progenitor cells. *Blood* **115:**1238–1246; 2010.
[14] Hosokawa, K.; Arai, F.; Yoshihara, H.; Nakamura, Y.; Gomei, Y.; Iwasaki, H.; Miyamoto, K.; Shima, H.; Ito, K.; Suda, T. Function of oxidative stress in the regulation of hematopoietic stem cell–niche interaction. *Biochem. Biophys. Res. Commun.* **363:** 578–583; 2007.
[15] Ito, K.; Hirao, A.; Arai, F.; Takubo, K.; Matsuoka, S.; Miyamoto, K.; Ohmura, M.; Naka, K.; Hosokawa, K.; Ikeda, Y.; Suda, T. Reactive oxygen species act through p38 MAPK to limit the lifespan of hematopoietic stem cells. *Nat. Med.* **12:** 446–451; 2006.
[16] Jang, Y. Y.; Sharkis, S. J. A low level of reactive oxygen species selects for primitive hematopoietic stem cells that may reside in the low-oxygenic niche. *Blood* **110:** 3056–3063; 2007.
[17] Miyamoto, K.; Araki, K. Y.; Naka, K.; Arai, F.; Takubo, K.; Yamazaki, S.; Matsuoka, S.; Miyamoto, T.; Ito, K.; Ohmura, M.; Chen, C.; Hosokawa, K.; Nakauchi, H.; Nakayama, K.; Nakayama, K. I.; Harada, M.; Motoyama, N.; Suda, T.; Hirao, A. Foxo3a is essential for maintenance of the hematopoietic stem cell pool. *Cell Stem Cell* **1:**101–112; 2007.
[18] Schraml, E.; Fuchs, R.; Kotzbeck, P.; Grillari, J.; Schauenstein, K. Acute adrenergic stress inhibits proliferation of murine hematopoietic progenitor cells via p38/MAPK signaling. *Stem Cells Dev.* **18:**215–227; 2009.

[19] Sheng, K. C.; Pietersz, G. A.; Tang, C. K.; Ramsland, P. A.; Apostolopoulos, V. Reactive oxygen species level defines two functionally distinctive stages of inflammatory dendritic cell development from mouse bone marrow. *J. Immunol.* **184:**2863–2872; 2010.

[20] Wang, Y.; Kellner, J.; Liu, L.; Zhou, D. Inhibition of p38 mitogen-activated protein kinase promotes ex vivo hematopoietic stem cell expansion. *Stem Cells Dev.* **20:** 1143–1152; 2011.

[21] Cuenca, A. G.; Delano, M. J.; Kelly-Scumpia, K. M.; Moreno, C.; Scumpia, P. O.; Laface, D. M.; Heyworth, P. G.; Efron, P. A.; Moldawer, L. L. A paradoxical role for myeloid-derived suppressor cells in sepsis and trauma. *Mol. Med.* **17:** 281–292; 2011.

[22] Diaz-Montero, C. M.; Salem, M. L.; Nishimura, M. I.; Garrett-Mayer, E.; Cole, D. J.; Montero, A. J. Increased circulating myeloid-derived suppressor cells correlate with clinical cancer stage, metastatic tumor burden, and doxorubicin–cyclophosphamide chemotherapy. *Cancer Immunol. Immunother.* **58:**49–59; 2009.

[23] Gabrilovich, D. I.; Nagaraj, S. Myeloid-derived suppressor cells as regulators of the immune system. *Nat. Rev. Immunol.* **9:**162–174; 2009.

[24] Greten, T. F.; Manns, M. P.; Korangy, F. Myeloid derived suppressor cells in human diseases. *Int. Immunopharmacol.* **11:**802–807; 2011.

[25] Haile, L. A.; von Wasielewski, R.; Gamrekelashvili, J.; Kruger, C.; Bachmann, O.; Westendorf, A. M.; Buer, J.; Liblau, R.; Manns, M. P.; Korangy, F.; Greten, T. F. Myeloid-derived suppressor cells in inflammatory bowel disease: a new immunoregulatory pathway. *Gastroenterology* **135:**871–881; 2008.

[26] Hoechst, B.; Ormandy, L. A.; Ballmaier, M.; Lehner, F.; Kruger, C.; Manns, M. P.; Greten, T. F.; Korangy, F. A new population of myeloid-derived suppressor cells in hepatocellular carcinoma patients induces CD4(+)CD25(+)Foxp3(+) T cells. *Gastroenterology* **135:**234–243; 2008.

[27] Hoechst, B.; Voigtlaender, T.; Ormandy, L.; Gamrekelashvili, J.; Zhao, F.; Wedemeyer, H.; Lehner, F.; Manns, M. P.; Greten, T. F.; Korangy, F. Myeloid derived suppressor cells inhibit natural killer cells in patients with hepatocellular carcinoma via the NKp30 receptor. *Hepatology* **50:**799–807; 2009.

[28] Marigo, I.; Dolcetti, L.; Serafini, P.; Zanovello, P.; Bronte, V. Tumor-induced tolerance and immune suppression by myeloid derived suppressor cells. *Immunol. Rev.* **222:** 162–179; 2008.

[29] Ostrand-Rosenberg, S.; Sinha, P. Myeloid-derived suppressor cells: linking inflammation and cancer. *J. Immunol.* **182:**4499–4506; 2009.

[30] Zhao, F.; Obermann, S.; von Wasielewski, R.; Haile, L.; Manns, M. P.; Korangy, F.; Greten, T. F. Increase in frequency of myeloid-derived suppressor cells in mice with spontaneous pancreatic carcinoma. *Immunology* **128:**141–149; 2009.

[31] Jenderny, S.; Lin, H.; Garrett, T.; Tew, K. D.; Townsend, D. M. Protective effects of a glutathione disulfide mimetic (NOV-002) against cisplatin induced kidney toxicity. *Biomed. Pharmacother.* **64:**73–76; 2010.

[32] Townsend, D. M.; Findlay, V. L.; Tew, K. D. Glutathione *S*-transferases as regulators of kinase pathways and anticancer drug targets. *Methods Enzymol.* **401:**287–307; 2005.

[33] Townsend, D. M.; He, L.; Hutchens, S.; Garrett, T. E.; Pazoles, C. J.; Tew, K. D. NOV-002, a glutathione disulfide mimetic, as a modulator of cellular redox balance. *Cancer Res.* **68:**2870–2877; 2008.

[34] Townsend, D. M.; Tew, K. D. Pharmacology of a mimetic of glutathione disulfide, NOV-002. *Biomed. Pharmacother.* **63:**75–78; 2009.

[35] Uys, J. D.; Manevich, Y.; Devane, L. C.; He, L.; Garret, T. E.; Pazoles, C. J.; Tew, K. D.; Townsend, D. M. Preclinical pharmacokinetic analysis of NOV-002, a glutathione disulfide mimetic. *Biomed. Pharmacother.* **64:**493–498; 2010.

[36] Townsend, D. M.; Pazoles, C. J.; Tew, K. D. NOV-002, a mimetic of glutathione disulfide. *Expert Opin. Investig. Drugs* **17:**1075–1083; 2008.

[37] Meng, A.; Wang, Y.; Brown, S. A.; Van Zant, G.; Zhou, D. Ionizing radiation and busulfan inhibit murine bone marrow cell hematopoietic function via apoptosis-dependent and -independent mechanisms. *Exp. Hematol.* **31:**1348–1356; 2003.

[38] Ploemacher, R. E.; van der Sluijs, J. P.; Voerman, J. S.; Brons, N. H. An in vitro limiting-dilution assay of long-term repopulating hematopoietic stem cells in the mouse. *Blood* **74:**2755–2763; 1989.

[39] Ploemacher, R. E.; van Os, R.; van Beurden, C. A.; Down, J. D. Murine haemopoietic stem cells with long-term engraftment and marrow repopulating ability are more resistant to γ-radiation than are spleen colony forming cells. *Int. J. Radiat. Biol.* **61:** 489–499; 1992.

[40] Diaz-Montero, C. M.; PN; Onicescu, G.; Zhu, Y.; Verma, N.; Garrett-Mayer, E.; Schuhwerk, K. C.; Pazoles, C. J.; Glück, S.; Montero, A. J. Daily injections of the glutathione disulfide mimetic NOV-002 ameliorates hematologic toxicities from neoadjuvant chemotherapy in breast cancer patients enrolled in the NEO-NOVO trial, and significantly increases circulating dendritic cells. CTRC-AACR San Antonio Breast Cancer Symposium, Edition San Antonio. Abstract 2141; December 10–14, 2008, San Antonio, Texas.

[41] Honeychurch, J.; Glennie, M. J.; Illidge, T. M. Cyclophosphamide inhibition of anti-CD40 monoclonal antibody-based therapy of B cell lymphoma is dependent on CD11b+ cells. *Cancer Res.* **65:**7493–7501; 2005.

[42] Salem, M. L.; Al-Khami, A. A.; El-Naggar, S. A.; Diaz-Montero, C. M.; Chen, Y.; Cole, D. J. Cyclophosphamide induces dynamic alterations in the host microenvironments resulting in a Flt3 ligand-dependent expansion of dendritic cells. *J. Immunol.* **184:** 1737–1747; 2010.

[43] Salem, M. L.; Diaz-Montero, C. M.; Al-Khami, A. A.; El-Naggar, S. A.; Naga, O.; Montero, A. J.; Khafagy, A.; Cole, D. J. Recovery from cyclophosphamide-induced lymphopenia results in expansion of immature dendritic cells which can mediate enhanced prime-boost vaccination antitumor responses in vivo when stimulated with the TLR3 agonist poly(I:C). *J. Immunol.* **182:**2030–2040; 2009.

[44] Salem, M. L.; El-Naggar, S. A.; Cole, D. J. Cyclophosphamide induces bone marrow to yield higher numbers of precursor dendritic cells in vitro capable of functional antigen presentation to T cells in vivo. *Cell. Immunol.* **261:**134–143; 2010.

[45] Salem, M. L.; Kadima, A. N.; El-Naggar, S. A.; Rubinstein, M. P.; Chen, Y.; Gillanders, W. E.; Cole, D. J. Defining the ability of cyclophosphamide preconditioning to enhance the antigen-specific CD8 + T-cell response to peptide vaccination: creation of a beneficial host microenvironment involving type I IFNs and myeloid cells. *J. Immunother.* **30:**40–53; 2007.

[46] Pelaez, B.; Campillo, J. A.; Lopez-Asenjo, J. A.; Subiza, J. L. Cyclophosphamide induces the development of early myeloid cells suppressing tumor cell growth by a nitric oxide-dependent mechanism. *J. Immunol.* **166:**6608–6615; 2001.

[47] Serafini, P.; Borrello, I.; Bronte, V. Myeloid suppressor cells in cancer: recruitment, phenotype, properties, and mechanisms of immune suppression. *Semin. Cancer Biol.* **16:**53–65; 2006.

[48] Crawford, J.; Dale, D. C.; Lyman, G. H. Chemotherapy-induced neutropenia: risks, consequences, and new directions for its management. *Cancer* **100:**228–237; 2004.

[49] Lu, Y.; Cederbaum, A. The mode of cisplatin-induced cell death in CYP2E1-overexpressing HepG2 cells: modulation by ERK, ROS, glutathione, and thioredoxin. *Free Radic. Biol. Med.* **43:**1061–1075; 2007.

[50] Martins, N. M.; Santos, N. A.; Curti, C.; Bianchi, M. L.; Santos, A. C. Cisplatin induces mitochondrial oxidative stress with resultant energetic metabolism impairment, membrane rigidification and apoptosis in rat liver. *J. Appl. Toxicol.* **28:**337–344; 2008.

[51] Pratheeshkumar, P.; Kuttan, G. Ameliorative action of Vernonia cinerea L. on cyclophosphamide-induced immunosuppression and oxidative stress in mice. *Inflammopharmacology* **18:**197–207; 2010.

[52] Asmis, R.; Wang, Y.; Xu, L.; Kisgati, M.; Begley, J. G.; Mieyal, J. J. A novel thiol oxidation-based mechanism for adriamycin-induced cell injury in human macrophages. *FASEB J.* **19:**1866–1868; 2005.

[53] Pratheeshkumar, P.; Kuttan, G. Cardiospermum halicacabum inhibits cyclophosphamide induced immunosuppression and oxidative stress in mice and also regulates iNOS and COX-2 gene expression in LPS stimulated macrophages. *Asian Pac. J. Cancer Prev.* **11:**1245–1252; 2010.

[54] Durken, M.; Agbenu, J.; Finckh, B.; Hubner, C.; Pichlmeier, U.; Zeller, W.; Winkler, K.; Zander, A.; Kohlschutter, A. Deteriorating free radical-trapping capacity and antioxidant status in plasma during bone marrow transplantation. *Bone Marrow Transplant.* **15:**757–762; 1995.